This article was downloaded by: [University Of Gujrat]
On: 11 December 2014, At: 13:52
Publisher: Taylor & Francis
Informa Ltd Registered in England and Wales Registered Number: 1072954 Registered office: Mortimer House, 37-41 Mortimer Street, London W1T 3JH, UK

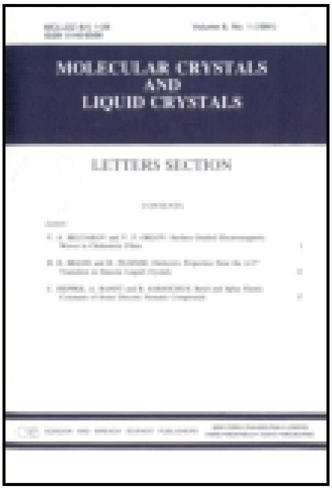

Molecular Crystals and Liquid Crystals
Publication details, including instructions for authors and subscription information:
http://www.tandfonline.com/loi/gmcl20

# Analysis of Structural and Electrical Properties of Solution-Processed Zinc Oxide Films for Thin-Film Transistor Application

Jin-Hyuk Bae[a], Jae Eun Hwang[b], Hong Doo Kim[b], Xue Zhang[c] & Jaehoon Park[c]

[a] School of Electronics Engineering, Kyungpook National University, Daegu, Republic of Korea

[b] Department of Advanced Materials Engineering for Information and Electronics, Kyung Hee University, Youngin, Republic of Korea

[c] Department of Electronic Engineering, Hallym University, Chuncheon, Republic of Korea

Published online: 17 Nov 2014.

To cite this article: Jin-Hyuk Bae, Jae Eun Hwang, Hong Doo Kim, Xue Zhang & Jaehoon Park (2014) Analysis of Structural and Electrical Properties of Solution-Processed Zinc Oxide Films for Thin-Film Transistor Application, Molecular Crystals and Liquid Crystals, 600:1, 28-34, DOI: 10.1080/15421406.2014.936545

To link to this article: http://dx.doi.org/10.1080/15421406.2014.936545

PLEASE SCROLL DOWN FOR ARTICLE

Taylor & Francis makes every effort to ensure the accuracy of all the information (the “Content”) contained in the publications on our platform. However, Taylor & Francis, our agents, and our licensors make no representations or warranties whatsoever as to the accuracy, completeness, or suitability for any purpose of the Content. Any opinions and views expressed in this publication are the opinions and views of the authors, and are not the views of or endorsed by Taylor & Francis. The accuracy of the Content should not be relied upon and should be independently verified with primary sources of information. Taylor and Francis shall not be liable for any losses, actions, claims, proceedings, demands, costs, expenses, damages, and other liabilities whatsoever or howsoever caused arising directly or indirectly in connection with, in relation to or arising out of the use of the Content.

This article may be used for research, teaching, and private study purposes. Any substantial or systematic reproduction, redistribution, reselling, loan, sub-licensing, systematic supply, or distribution in any form to anyone is expressly forbidden. Terms &

*Mol. Cryst. Liq. Cryst.*, Vol. 600: pp. 28–34, 2014
Copyright © Taylor & Francis Group, LLC
ISSN: 1542-1406 print/1563-5287 online
DOI: 10.1080/15421406.2014.936545

# Analysis of Structural and Electrical Properties of Solution-Processed Zinc Oxide Films for Thin-Film Transistor Application

JIN-HYUK BAE,[1,†] JAE EUN HWANG,[2,†] HONG DOO KIM,[2]
XUE ZHANG,[3] AND JAEHOON PARK[3,*]

[1]School of Electronics Engineering, Kyungpook National University, Daegu, Republic of Korea
[2]Department of Advanced Materials Engineering for Information and Electronics, Kyung Hee University, Youngin, Republic of Korea
[3]Department of Electronic Engineering, Hallym University, Chuncheon, Republic of Korea

*We investigated the electrical properties of solution-processed zinc oxide (ZnO) thin-film transistors (TFTs) with varying the size of ZnO crystallites in the film. The TFTs having the bead-shaped ZnO crystallites with the average diameter of 2 μm apparently operated in depletion mode, whereas the devices exhibited an accumulation operation when the crystallite size of ZnO reduced to sub-micron range. Considering the difference between bulk and channel electrical conductivities in solution-processed ZnO TFTs, these results are explained with the interplay between the crystallite size of ZnO and the electrical conduction in the TFT.*

**Keywords** Oxide semiconductor; thin-film transistor; channel conductivity; bulk conductivity; charge trap

## Introduction

Oxide semiconductors have emerged as an alternative material for silicon and organic semiconductors [1−3]. In particular, zinc oxide (ZnO) thin-film transistors (TFTs) have attracted much attention in recent years due to their good electrical properties and excellent ambient stability. It should be also recognized that the optical transparency of ZnO films is inherently advantageous for see-through electronic devices. Many researchers have thus reported that various processes involving high deposition temperatures and post-annealing treatments can produce transparent amorphous oxide semiconductor TFTs with good electric characteristics and stability [4, 5]. For example, ZnO thin films have mostly been produced by means of vacuum deposition methods, such as sputtering and pulsed laser deposition techniques [6, 7]. However, solution processes utilizing sol-gel precursors are more viable for

---

[†] These authors contributed equally to this work.

[*] Address correspondence to Prof. Jaehoon Park, 1 Hallymdaehak-gil, Chuncheon, Gangwon-do, 200-702, Korea. Tel.: +82-33-248-2357; Fax: +82-33-242-2352. E-mail: jaypark@hallym.ac.kr

Color versions of one or more of the figures in the article can be found online at www.tandfonline.com/gmcl.

applications in flexible electronics because they allow the possibility of significant cost reduction via mass-manufacturing roll-to-roll processes using a combination of conventional coating and printing techniques. As the solidification of a solution-processed oxide semiconductor is essentially distinguished from the growth kinetics of vacuum-deposited films, the structural effects of solution-processed oxide semiconducting films on the electrical characteristics of these TFTs should be comprehensively studied.

In this work, we report the underlying effect of the crystallite size of solution-processed ZnO on the electrical characteristics of ZnO TFTs. Bottom-contact structured ZnO TFTs were fabricated with varying the size of ZnO crystallites in the film. The bulk and channel electrical conductivities in these TFTs are considered to demonstrate the interplay between the crystallite size of ZnO and the electrical conduction in the TFT.

## Experimental

The precursor solution for the ZnO film was prepared in ambient air by dissolving ZnO particles (99.99%, Sigma Aldrich) in $NH_4OH$ (25∼30%, Duksan) to be about 0.9 wt.%. To make the precursor solution stable, it was placed in a refrigerator for 12 h after stirring using a magnetic bar for 1 h. For the fabrication of bottom-contact and bottom-gate TFT structure, 50-nm-thick Al source and drain electrodes were thermally evaporated onto the 100-nm-thick $SiO_2$/p+-Si substrate using a shadow mask; the base pressure was maintained under $1.6\times10^{-6}$ Torr. The channel width and length for the fabricated device are 400 and 50 $\mu$m, respectively. The mixed precursor solution was filtered through a 0.45-$\mu$m syringe filter and was then deposited on the substrate via drop-casting or spin-coating at 3000 rpm for 30 s; the substrate was kept at room temperature during the deposition of ZnO films. To remove the solvent, we heated the substrate at 150°C for 30 min by using a hot plate. Here, the deposition and thermal curing for ZnO films were processed in ambient air. Finally, Ag paste was then attached on the silicon substrate to provide the contact electrode for the bottom gate.

The structural properties of solution-processed ZnO films were investigated using X-ray diffraction (XRD, X'pert pro, Panalytical) and X-ray photoelectron spectroscopy (XPS, Theta Probe AR-XPS system, Thermo Fisher Scientific). The surface characteristics of films were analyzed with atomic force microscopy (AFM, XE-150, PSIA). Electrical characterizations of the fabricated ZnO TFTs were performed in the dark and in ambient air using a semiconductor analyzer (4200, Keithley).

## Results and Discussion

Figure 1(a) shows the optical transmission spectrum in the wavelength range from 300 to 800 nm for the drop-casted ZnO film on a quartz substrate. The film exhibits a transmittance value of above 90 % in the visible spectral range between 400 and 800 nm. Such an optical transparency is known to be advantageous for applications in see-through electronic devices. The band gap energy ($E_g$) of the ZnO film can be calculated by assuming that $(\alpha h\nu)^2 \propto (h\nu - E_g)$, where $\alpha$ is the absorption coefficient and $h\nu$ is the photon energy [8]; the absorption coefficient is determined by $\alpha = [2.303 \times \log(1/T)]/d$, where $T$ is the transmittance and $d$ is the film thickness. The band gap energy of the fabricated ZnO film in this study is determined to be approximately 3.4 eV, which is close to the values reported in the literature [9]. Figure 1(b) shows the XRD peaks for the drop-casted ZnO film. The characteristic peak near 34.6° indicates the c-axis-oriented (002) plane in our ZnO film and two shoulder

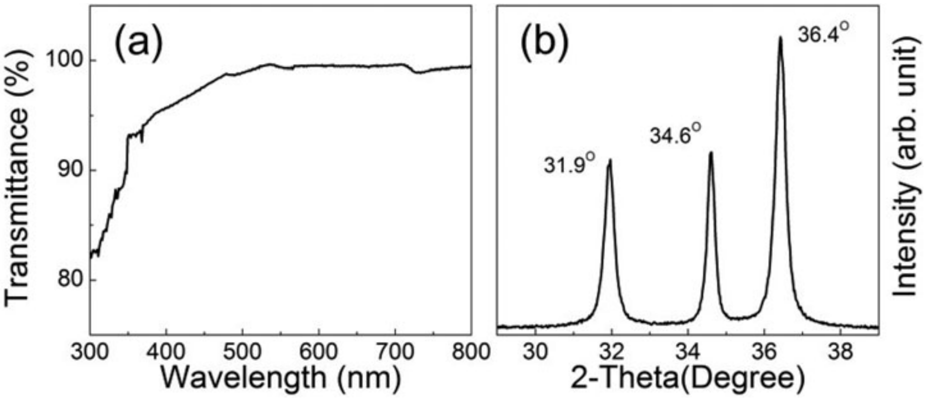

Figure 1. (a) Optical transmittance and (b) XRD spectrum of the drop-casted ZnO film.

peaks at around 31.9° and 36.4° correspond to additional (100) and (101) orientations in the film. These three different diffraction peaks suggest a typical wurzite hexagonal bulk ZnO structure [10].

Figure 2(a) shows the optical microscope image of the drop-casted ZnO film, in which the average diameter of bead-shaped ZnO crystallites is determined to be approximately 2 $\mu$m; the film thickness was approximately 5 $\mu$m. Although ZnO crystallites are densely condensed together, there is a critical discontinuity in the film, i.e. voids or cracks. Figure 2(b) shows the drain current ($I_D$) versus drain voltage ($V_D$) curves of the drop-casted ZnO TFT. Noteworthy is that the drain currents of the drop-casted transistor significantly

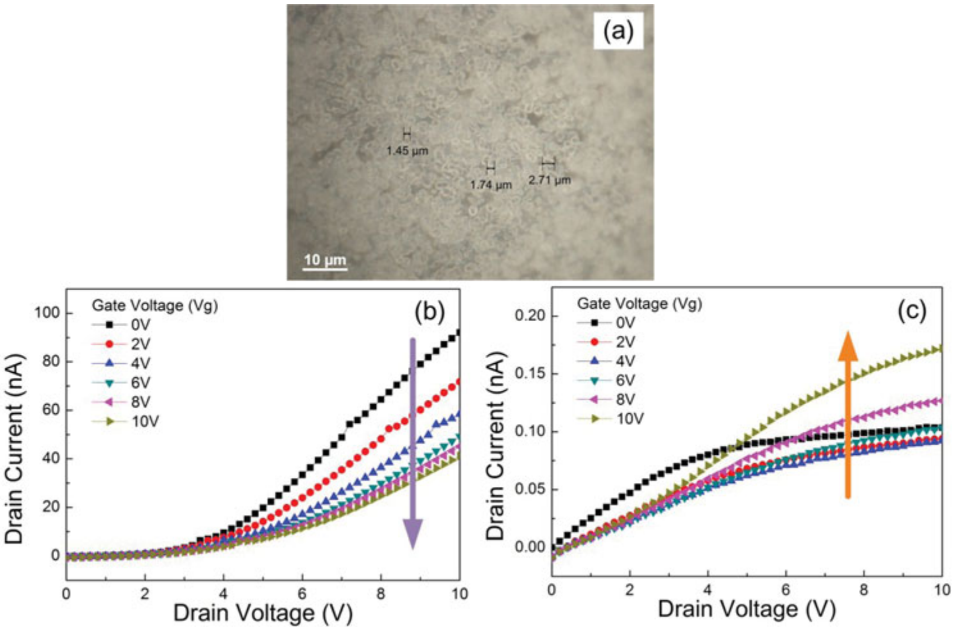

Figure 2. (a) Optical microscope image of the drop-casted ZnO film. Output characteristics of the drop-casted ZnO TFT, which were measured (b) as fabricated and (c) after device storage in air.

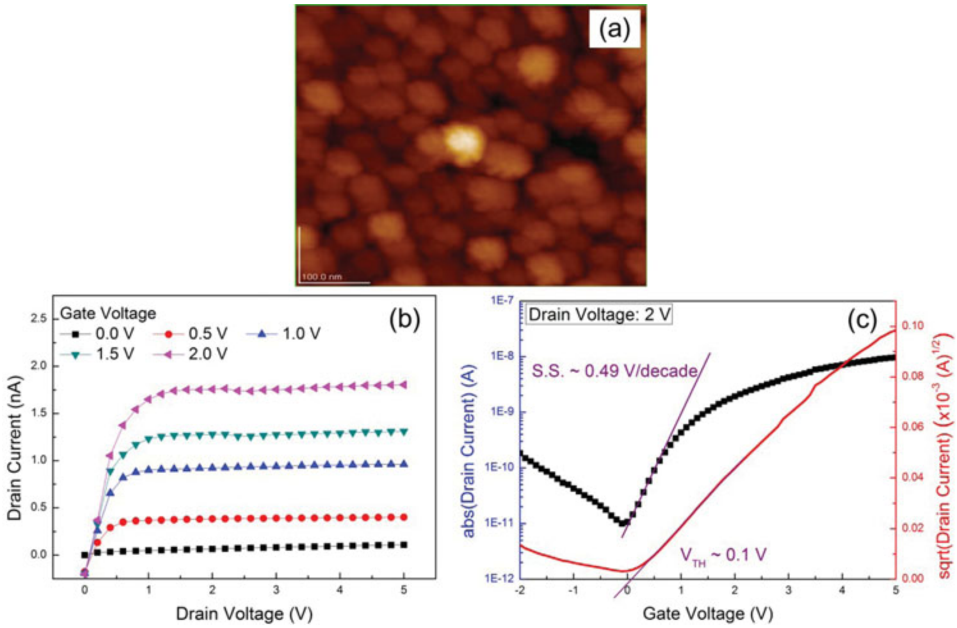

**Figure 3.** AFM image of the spin-coated ZnO film. (b) Output and (c) transfer characteristics of the spin-coated ZnO TFT.

decreased with increasing the gate voltage ($V_G$); the device apparently operated in depletion mode. The result is a striking contrast to the electrical characteristics of ZnO TFTs reported in literature [11, 12]; ZnO TFTs exhibit an *n*-channel behavior operating in accumulation mode on a positive gate bias. However, it is interesting that the drop-casted ZnO TFT operated in accumulation mode after device storage in air for 5 hr, as shown in Fig. 2(c). Compared to the electrical characteristics of the as-fabricated device in Fig. 2(b), the notable decrease in the drain current after device storage in air, as shown in Fig. 2(c), is indicative of the decrease in the electrical conductivity at the bulk of the drop-casted ZnO film. This characteristic change might be owing to the influence of ambient molecules on the electrical conduction in ZnO TFTs because our TFTs were not passivated [13, 14].

The AFM image ($0.5\ \mu$m $\times$ $0.5\ \mu$m) of the surface morphology of the spin-coated ZnO film is shown in Fig. 3(a); the thickness of the spin-cated ZnO films was about 20 nm. The average diameter of spin-coated ZnO crystallites in the spin-coated film was approximately 60 nm and the average surface roughness was approximately 1.2 nm. It is clear that the spin-coating method produced much smaller ZnO crystallites than those deposited via the drop-casting method. As shown in Fig. 3(b), the spin-coated ZnO TFT exhibited clear pinch-off and excellent saturation behavior operated in accumulation mode. The drain currents of the spin-coated ZnO TFT somehow intervened between the two results shown in Figs. 2(b) and 2(c), which implies both the dependence of charge transport behavior on the ZnO crystallite size and the significance of the structural continuity in the solution-processed ZnO film. It should be reminded that the drop-casted ZnO film exhibited bead-shaped crystallites with an average diameter of $2\ \mu$m and structural discontinuities as shown in Fig. 2(a). Herein, important device properties are extracted from the transfer characteristic plots of $\log_{10}|I_D|$-$V_G$ and $|I_D|^{1/2}$-$V_G$ at a positive $V_D$ of 2 V, shown in Fig. 3(c). From the transfer curves, the field-effect mobility in the saturation region is theoretically

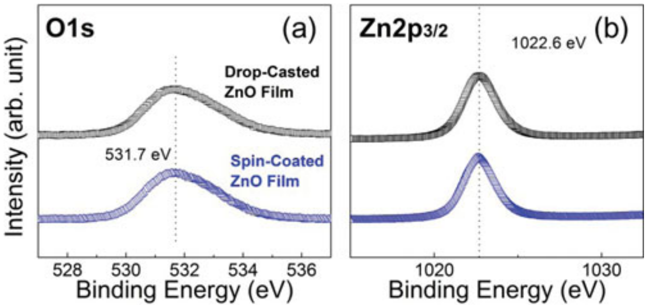

**Figure 4.** Comparison of the (a) O 1s and (b) Zn $2p_{3/2}$ core level spectra obtained from drop-casted and spin-coated ZnO films.

given by

$$I_D = \frac{W}{2L} C_i \mu_{sat} (V_G - V_T)^2,$$

where $L$ and $W$ are the channel length and width, respectively [15]. Here, $C_i$ is the capacitance per unit area of the gate insulator (46 nF in this study), $\mu_{sat}$ is the field-effect mobility in the saturation region, $V_G$ is the gate voltage, and $V_T$ is the threshold voltage. The spin-coated ZnO TFT exhibited a field-effect mobility of 0.04 cm$^2$/Vs, a threshold voltage of 0.1 V, a current on/off ratio of $10^3$, and a subthreshold swing of 0.49 V/decade. Considering the influence of channel layer thickness on the electrical performances in oxide TFTs [16], the relatively low field-effect mobility and current values in the results can be attributed to the thin thickness of the spin-coated ZnO films.

We now discuss the conflict of the electrical characteristics in the fabricated ZnO TFTs. The XPS results of drop-casted and spin-coated ZnO films are compared to identify the change in their chemical structure. In this study, prior to the XPS measurements, *in-situ* $Ar^+$ ion etching with 10 nm/min was performed to avoid any surface contamination. Therefore, the present XPS spectra were likely to originate from the inside of the film rather than the film surface. Note that it was not possible to measure the bottom-side characteristics of ZnO films near the substrate because the brittle films could not be detached. As shown in Figs. 4(a) and 4(b), there were no discernible shifts in O 1s and Zn $2p_{3/2}$ core level spectra. For both ZnO films, the maximum binding energies of O 1s and Zn $2p_{3/2}$ remain at 531.7 eV and 1022.6 eV, respectively. This indicates that a large majority of Zn atoms remained, in all probed films, in the same formal valence state of $Zn^{2+}$ within an oxygen-deficient ZnO matrix and the concentration of oxygen vacancies was not affected by the deposition method. Therefore, the difference in the electrical characteristics of drop-casted and spin-coated ZnO TFTs can be attributed to the morphological properties of solution-processed ZnO films. Note that the diameters of drop-casted and spin-coated ZnO crystallites are 2 $\mu$m and 60 nm. Figure 5 depicts possible pathways for the charge transport in the drop-casted ZnO TFT; in this proposed model, the electrical conduction is assumed to occur through the bulk of the ZnO film and at the ZnO/gate insulator (GI) interface. When the gate voltage is not applied, the drain current depends on the drain voltage, suggesting that the bulk conduction would dominate the current flow through the drop-casted ZnO film. On the other hand, an amount of electrons will accumulate at the ZnO/GI interface under the influence of positive gate bias. In this case, the morphological discontinuity produced by micron-size ZnO particles may act as charge-trapping sites, thereby deteriorating the

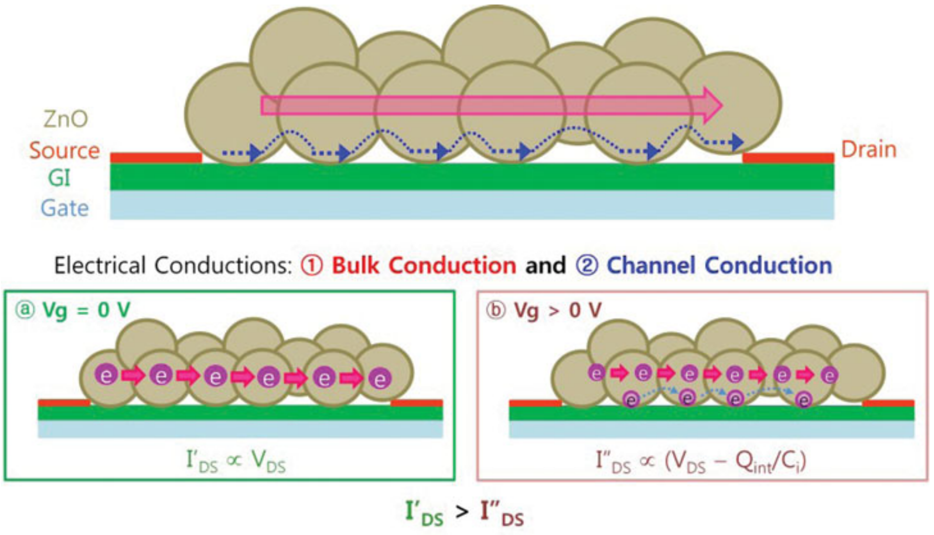

**Figure 5.** Electrical conduction model in the drop-casted ZnO TFT.

electrical characteristics of the TFT. As the accumulation electrons at the ZnO/GI interface depend on the applied gate bias, more electrons can be trapped with increasing the gate voltage; the trapped charge density is denoted as $Q_{ins}$ in Fig. 5. This explains the reason for that the drop-casted ZnO TFTs apparently operated in depletion mode [Fig. 2(b)]. The characteristic recovery, which was observed in the drop-casted TFT after device storage in air [Fig. 2(c)], is thought to be related with the reduction of the bulk conductivity as a consequence of permeation of air molecules into the drop-casted ZnO film through structural defects, such as voids or cracks [14, 17]. In other words, when the electrical conductivity in the drop-casted ZnO bulk gets lowered and thus becomes comparable to that in the channel region of the TFT, the drain current possibly increases with increasing the gate voltage. The fact that the spin-coated ZnO TFTs with sub-micron-sized ZnO crystals operated in a typical accumulation mode also suggests a significant interplay between the crystallite size of solution-processed ZnO and the electrical conduction in the TFT.

## Conclusion

We fabricated solution-processed ZnO TFTs with a bottom-contact and bottom-gate structure. The ZnO films were deposited by means of drop-casting and spin-coating methods. For the case of the drop-casted TFTs having the bead-shaped ZnO crystallites with the average diameter of 2 $\mu$m, the drain currents rather decreased with increasing the gate voltage; the device apparently operated in depletion mode. On the other hand, the TFTs exhibited clear pinch-off and excellent saturation behavior with an accumulation operation when the crystallite size of ZnO in the film reduced to sub-micron range (approximately 60 nm in this study). The conflict of the TFT characteristics in this study could be explained by the interplay between the crystallite size of ZnO and the electrical conduction in the TFT. Consequently, we can conclude that the packing density of solution-processed ZnO crystals is of prime importance for the performance of these TFTs. Further quantitative analyses on the relation between the structural defects in solution-processes oxide films and the trapped charge density in TFTs still remain to be carried out.

## Funding

This research was supported by Hallym University Research Fund, 2014(HRF-2014) and the research project (10041808) funded by the Ministry of Knowledge Economy (MKE) of the Korean Government.

## References

[1] Gelinck, G., Heremans, P., Nomoto, K., & Anthopoulos, T. D. (2010). *Adv. Mater. 22*, 3778.

[2] Street, R. A. (2009). *Adv. Mater. 21*, 2007.

[3] Bashir, A., Wöbkenberg, P. H., Smith, J., Ball, J. M., Adamopoulos, G., Bradley, D. D. C., & Anthopoulos, T. D. (2009). *Adv. Mater. 21*, 2226.

[4] Matsuda, T., Furuta, M., Hiramatsu, T., Furuta, H., & Hirao, T. (2010). *J. Vac. Sci. Technol. A. 28*, 135.

[5] Hirao, T., Furuta, M., Hiramatsu, T., Matsuda, T., Chaoyang, L., Furuta, H., Hokari, H., Yoshida, M., Ishii, H., & Kakegawa, M. (2008). *IEEE Trans. Electron Devices 55*, 3136.

[6] Ellmer, K. (2000). *J. Phys. D: Appl. Phys. 33*, R17.

[7] Bayraktaroglu, B., & Leedy, K. (2008). *ECS Transactions 16*, 61.

[8] Bang, S., Lee, S., Jeon, S., Kwon, S., Jeong, W., Kim, H., Shin, I., Chang, H. J., Park, H.-H., & Jeon, H. (2009). *Semicond. Sci. Technol. 24*, 025008.

[9] Srikant, V., & Clarke, D. R. (1998). *J. Appl. Phys. 83*, 5447.

[10] Lee, G. H., Yamamoto, Y., Kourogi, M., & Ohtsu, M. (2001). *Thin Solid Films 386*, 117.

[11] Ong, B. S., Li, C., Li, Y., Wu, Y., & Loutfy, R. (2007). *J. Am. Chem. Soc. 129*, 2751.

[12] Bong, H., Lee, W. H., Lee, D. Y., Kim, B. J., Cho, J. H., & Cho, K. W. (2010). *Appl. Phys. Lett. 96*, 192115.

[13] Levy, D. H., Freeman, D., Nelson, S. F., Cowdery-Corvan, P. J., & Irving, L. M. (2008). *Appl. Phys. Lett. 92*, 192101.

[14] Chen, W.-T., Lo, S.-Y., Kao, S.-C., Zan, H.-W., Tsai, C.-C., Lin, J.-H., Fang, C.-H., & Lee, C.-C. (2011). *IEEE Electron Device Lett. 32*, 1552.

[15] Dimitrakopoulos, C. D., & Mascaro, D. J. (2001). *IBM J. Res. Dev. 45*, 11.

[16] Wang, Y., Sun, X. W., Goh, G. K. L., Demir, H. V., & Yu, H. Y. (2011). *IEEE Trans. Electron Devices 58*, 480.

[17] Jeong, J. K., Yang, H. W., Jeong, J. H., Mo, Y.-G., & Kim, H. D. (2008). *Appl. Phys. Lett. 93*, 123508.